Desalination and Water Treatment
www.deswater.com

doi: 10.5004/dwt.2022.28126

248 (2022) 259–267
February

Degradation of acesulfame by ultraviolet-activated peroxymonosulfate: role of sulfate and hydroxyl radicals

Honghai Xue[a], Jinying Li[a], Siyu Gao[a,b], Binshuo Liu[c], Wenbo Zhu[a], Chunqing Wang[d,*], Ming Li[a,*]

[a]*Key Laboratory of Songliao Aquatic Environment, Ministry of Education, Jilin Jianzhu University, Changchun 130118, China, emails: mgvi@163.com (M. Li), xuehonghai@jlju.edu.cn (H. Xue), 1986472643@qq.com (J. Li), 457865183@qq.com (S. Gao), 3100556783@qq.com (W. Zhu)*
[b]*New World Architectural Design Co., Ltd., Shenyang 110179, China*
[c]*Disciplines Construction Office, Jilin Jianzhu University, Changchun 130118, China, email: liubinshuo73@163.com*
[d]*Key Laboratory for Comprehensive Energy Saving of Cold Regions Architecture, Ministry of Education, Jilin Jianzhu University, Changchun 130118, China, email: wangchunqing@jlju.edu.cn*

Received 28 July 2021; Accepted 30 December 2021

ABSTRACT

Among the most typical artificial sweeteners, acesulfame (ACE) is now ubiquitously detected in aquatic environments. The degradation of ACE by ultraviolet (UV)-activated peroxymonosulfate (PMS) process was systematically investigated. ACE degradation via UV/PMS fits the pseudo-first-order kinetics. 97.63% degradation of ACE (4.78 μM) was achieved after 24 min of treatment with 25 μM PMS. Compared with the neutral pH condition (pH = 7.17), an acidic pH (pH = 2.75 or 5.03) weakly promoted the degradation of ACE, whereas an alkaline condition (pH = 10.90) significantly promoted it. Inorganic anions had varied effects on ACE degradation, with promoting effect of NO_3^- and inhibitory effects of HCO_3^- and Cl^-. ACE degradation was also reduced by the presence of humic acid and fulvic acid. Inhibitory effect on ACE degradation was also observed when the experiment was carried out in natural water. Four degradation by-products of ACE were identified and the degradation mechanisms were proposed. Hydroxyl radicals were identified as the primary contributor to ACE degradation based on quenching experiments. UV/PMS was more favorable than UV/H_2O_2 considering the degradation and mineralization efficiencies of ACE, although it was inferior to that of UV-activated peroxydisulfate.

Keywords: Acesulfame; Degradation; Mechanism; Peroxymonosulfate; Ultraviolet

1. Introduction

Artificial sweeteners (ASs), a class of emerging pollutants, are widely utilized as dietary supplements due to their high sweetness and low calories [1]. After ingestion, certain ASs pass through the human metabolism largely unaffected and can reach the domestic wastewater environment [2]. Several commonly used ASs exist in aquatic environments, such as acesulfame (ACE), sucralose, and saccharin [3]. Of these, ACE has been frequently detected in various water environment. For example, ACE was detected at 0.0013 μM (0.22 μg L^{-1}) in an open coastal system at an estuarine/marine junction in Hong Kong, China [4], at 0.016 μM (2.60 μg L^{-1}) in tap water from Switzerland [2], and about 0.25 μM (40 μg L^{-1}) in influents of two German sewage treatment plants [5].

ASs have received increasing attention due to their environmental persistence and harmful effects [6–8]. For example, Sang et al. [4] measured the acute toxicity of

---

* Corresponding authors.

ACE metabolites (with photo treatment) to *V. fischeri* and demonstrated that the biotoxicity of ACE metabolites was significantly amplified to 125.5 mg L^{-1} with a measurable magnification factor of 575 compared with the parent compound. Atrayee et al. [9] evaluated the genotoxic potential of ACE by comet assay in the bone marrow cells of mice, and found ACE can cause DNA damage. As conventional treatments may not substantially remove ASs, radical-based advanced oxidation processes (AOPs) can be a viable alternative [10]. Persulfate exhibits a high aqueous solubility, long lifetime, high stability in subsurface applications, and low cost [11,12]. Peroxydisulfate (PDS), activated by energy or a catalyst, is commonly used to produce sulfate radicals ($SO_4^{\bullet-}$) and has been widely studied [13]. Peroxymonosulfate (PMS) is an unsymmetrical oxidant that can be activated to generate both hydroxyl radicals ($^{\bullet}OH$) and $SO_4^{\bullet-}$ [Eq. (1)] [14–16].

$$HSO_5^- \xrightarrow{h\upsilon} SO_4^{\bullet-} + {}^{\bullet}OH \tag{1}$$

Similar to $^{\bullet}OH$ (2.74 V), $SO_4^{\bullet-}$ has comparable redox potential (2.5–3.1 V) [17,18]. It is also a strong oxidizing radical [19], and can initiate a series of radical chain reactions that degrade organic compounds [11]. What's more, $SO_4^{\bullet-}$ has wider operating pH range [20], functions in milder reaction conditions, and often leads to an increased mineralization degree [21].

PMS can easily be activated by various methods, including ultraviolet (UV) irradiation [22], heat [23], ultrasound [24], nanostructured carbons [25], transition metals [26,27], and ozone [8]. Of these methods, UV/PMS is considered a benign and economical technology [14]. Several attempts to degrade ACE based on $^{\bullet}OH$ and $SO_4^{\bullet-}$ have been employed. Li et al. [28] found that UV/PDS has advantages over UV/H_2O_2 in degrading ACE under the same experimental conditions. The degradation of ACE by UV/H_2O_2 was four times slower than that by UV/PDS in pure water. The degradation rate of ACE reduced in secondary effluent by both UV/PDS and UV/H_2O_2, but reduced less by UV/PDS than that by UV/H_2O_2, indicating the greater applicability of UV/PDS to real wastewater conditions. Recently, Wang et al. [29] investigated the removal performance of ACE (30 μM) under strong acid condition (pH = 3.0) by UV-LED (265 nm) activated PMS, the degradation rate of ACE after 120 min was 76% when PMS concentration was 188 μM.

Therefore, UV/PMS technology was adopted to degrade ACE under various pH conditions in this study. Initially, the reaction kinetics of ACE degradation by UV/PMS were established. Subsequently, the effects of operating parameters, including the initial concentration of ACE, the dosage of PMS, solution pH, inorganic ions, humic acid (HA), fulvic acid (FA), and water quality on the removal of ACE were studied. The transformation by-products of ACE were determined and the degradation mechanisms were revealed. The relative contributions of $^{\bullet}OH$ and $SO_4^{\bullet-}$ during ACE degradation were calculated based on quenching experiments. Finally, the ACE degradation and mineralization efficiencies of UV/PMS were compared with that of UV/PDS and UV/H_2O_2. The experimental results can help to guide the practical application of UV/PMS technology for treating ACE-containing water.

2. Experimental methods

2.1. ACE degradation methods

The degradation reaction of ACE ($C_4H_4KNO_4S$, Analytical-grade, TCI Huacheng Industrial Development Co., Ltd., Shanghai, China) was conducted in a photochemical reactor (PL-01, Beijing Prince Technology Co., Ltd., China), a mercury lamp (500 W) with a main emission wavelength of 365 nm and light intensity of 100 mW cm^{-2} was used as light source. The quartz tubes containing 40 ml mixed solution of ACE and PMS (Analytical-grade, Sigma-Aldrich, USA) were evenly distributed around the light source. The initial concentration of ACE was set about 5 μM, unless otherwise stated. More information about the photochemical reactor can be found in our previous study [30]. During the ACE degradation reaction, two parallel samples (0.5 mL) were periodically withdrawn for further analysis. The ACE concentration in the samples was immediately analyzed using HPLC after filtration with a 0.22 μm membrane. When required, HA, FA, $NaHCO_3$, NaCl, $NaNO_3$, H_2SO_4, NaOH, methanol (MeOH) and tert-butanol (TBA) were mixed with ACE before the reaction occurred.

2.2. ACE degradation in natural water

Surface water (SW) was sampled from the Xinlicheng Reservoir in Changchun, China, and the samples were filtered through a 0.45 μm nitrocellulose membrane and stored at a temperature of 4°C before use. The pH of the SW was 8.04, and the dissolved organic carbon content was 11.25 mg L^{-1}. ACE in SW was determined by high-performance liquid chromatography (HPLC), and no ACE was detected.

2.3. Analysis methods

An HPLC (1200 Series, Agilent, USA) was used to measure the ACE concentration in the treated solution. A Symmetry C18 column (5 μm, 4.6 mm × 150 mm, Waters, USA) was used with a 230 nm wavelength of a variable wavelength detector. The mobile phase was an 18:82 mixture of methanol and ammonium acetate solution (0.02 mol L^{-1}). The flow rate was 0.5 mL min^{-1}, and the injection volume was 10 μL.

The byproducts produced during ACE degradation process were determined by ultrahigh-performance liquid chromatography time-of-flight mass spectrometry (UPLC/TOF-MS). The total organic carbon (TOC) was determined by using a TOC-Vcph analyzer (Shimadzu, Japan). Detailed analysis methods for ACE and its degradation products, TOC, and pH value during ACE degradation were identical to our previous study [31]. The consumption of PMS during the degradation of ACE was determined by referring to previously reported method [32]. Each experiment was conducted twice, and the mean values with error bars were calculated and reported.

3. Results and discussion

3.1. Role of PMS dosage and ACE concentration

It is commonly assumed that in activated PMS systems, the increase of the relative amount of PMS would result in subsequent elevated generation of radicals, and thus could enhance the degradation rate of contaminants [33]. Fig. 1 demonstrates that the degradation of ACE was enhanced as the initial PMS concentration increased. As shown in Table 1, *k* increased from 0.0271 to 0.3509 min^{-1} when PMS concentration increased from 5 to 100 μM. This was because more $SO_4^{\bullet-}$ and $^{\bullet}OH$ could be produced (Eq. (1)) from high concentration PMS by UV activation, thus promoted the degradation of ACE. This was consistent with previous studies [34]. It was reported that when the PMS dosage exceeded the optimal dose, it may inhibit the degradation of pollutants, due to the self-quenching of $SO_4^{\bullet-}$ and $^{\bullet}OH$ by PMS [35]. However, within the PMS concentration range (5–100 μM) used in this experiment, the above phenomenon has not been observed. 97.63% ACE was degraded after 24 min of treatment with 25 μM of PMS. Therefore, 25 μM PMS was chosen for the following experiments, unless otherwise stated.

The PMS concentration was fixed at 25 μM, and the ACE degradation was investigated at various ACE concentrations (from 4.78 to 48.89 μM). Fig. 2 demonstrated that an increasing initial concentration of ACE significantly reduced its degradation. As shown in Table 1, *k* decreased from 0.1469 to 0.0297 min^{-1} when ACE concentration increased from 4.78 to 48.89 μM. This occurred because the amount of $SO_4^{\bullet-}$ and $^{\bullet}OH$ was constant at given PMS concentration. Thus, ACE degradation was reduced when increasing initial ACE concentration due to fewer radicals available per ACE molecule. In addition, high concentration of ACE resulted in increased formation/concentration of intermediates which in turn lowered the reaction rate of radicals towards ACE [15].

As shown in Table 1, ACE degradation at various initial PMS and ACE concentrations fits well with the first-order reaction kinetics ($R^2 > 0.9$). *k* increased with the increasing PMS concentration, but decreased with the increasing ACE concentration. Finally, 25 μM of PMS and 4.78 μM of ACE were regarded as optimal experimental condition, the ACE degradation rate was 0.1469 min^{-1}. Wang et al. [29] reported that the ACE degradation rate by UV/PMS was 0.012 min^{-1} under strong acid condition (pH = 3.0) when ACE and PMS concentration was 30 and 188 μM. After the degradation of ACE (24 min), the residual PMS concentration was 15.20 μM, indicating that PMS was excessive and only 39.20% of PMS was consumed. Of note, when 25 μM of PMS and 4.78 μM of ACE were mixed together and placed in the dark for 1 h (without UV), almost no loss of ACE (<1%) was

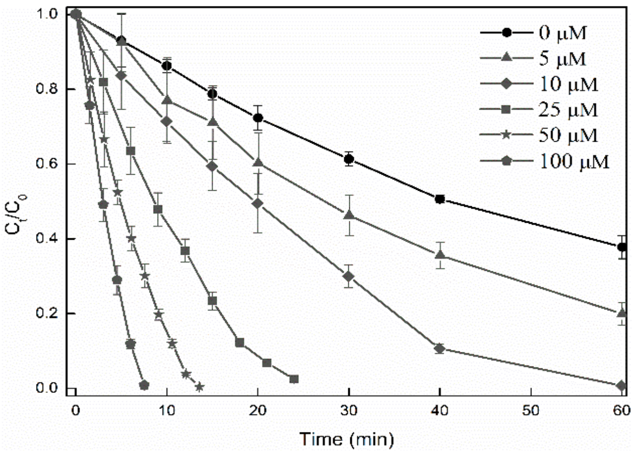

Fig. 1. Degradation of ACE by UV/PMS at different PMS dosage (average $[ACE]_0 = 4.85 \pm 0.014$ μM, PMS/ACE molar ratios was about 1–20).

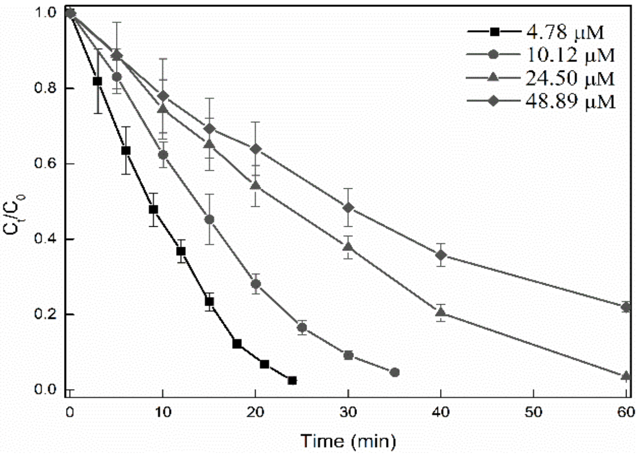

Fig. 2. Degradation of ACE by UV/PMS at different ACE concentration ($[PMS]_0 = 25$ μM) (PMS/ACE molar ratios was about 0.5–5.0).

Table 1
Kinetic parameters of ACE degradation by UV/PMS

ACE concentration (μM)	PMS concentration (μM)	*k* (min^{-1})	$t_{1/2}$ (min)	R^2
4.80	0	0.0170	40.77	0.9985
4.95	5	0.0271	25.58	0.9981
4.91	10	0.0529	13.10	0.9403
4.78	25	0.1469	4.72	0.9303
4.81	50	0.2395	2.89	0.9127
4.85	100	0.3509	1.98	0.9537
10.12	25	0.0878	7.89	0.9658
24.50	25	0.0536	12.93	0.9407
48.89	25	0.0297	23.34	0.9821

observed. Therefore, the loss due to dark reaction can be neglected.

3.2. Effect of solution pH

The pH value of the mixing solution (4.78 μM of ACE and 25 μM of PMS) was 5.03, and it was adjusted by sulfuric acid or sodium hydroxide. As can be seen from Fig. 3, compared with the neutral condition (pH = 7.17), both, the acidic (pH = 2.75 or 5.03) and alkaline (pH = 10.90) conditions, promoted ACE degradation. Liang and Su [36] reported that the predominant radical was $SO_4^{\bullet-}$ under acidic conditions; and $SO_4^{\bullet-}$ has a higher redox potential under acidic conditions [37]. Therefore, ACE degradation was promoted under acidic conditions. While the predominant radical became $^{\bullet}OH$ under a strong alkaline pH, and ACE was more reactive with $^{\bullet}OH$ [10]. Therefore, the promoting effect under alkaline conditions was particularly significant. Guan et al. [38] reported that the apparent molar absorption coefficient of PMS increased with pH from 13.8 to 149.5 M^{-1} cm^{-1} in the pH range of 6–12. Therefore, more $^{\bullet}OH$ and $SO_4^{\bullet-}$ can be generated under alkaline conditions, and ACE degradation was enhanced.

3.3. Relative contributions of reactive species

MeOH is an effective quencher of $SO_4^{\bullet-}$ and $^{\bullet}OH$, and TBA is a quencher of $^{\bullet}OH$, so they were used to distinguish the roles of $SO_4^{\bullet-}$ and $^{\bullet}OH$ [39]. Roles of MeOH and TBA on ACE degradation are shown in Fig. 4. ACE degradation was significantly reduced with the presence of TBA, suggesting the great contribution from $^{\bullet}OH$. However, no obvious difference in ACE degradation was observed in UV/PMS system with the presence of MeOH and TBA, indicating negligible role of $SO_4^{\bullet-}$. UV photolysis also contributed to ACE degradation, because ACE can absorb the ultraviolet light emitted by the light source used in this experiment. (Fig. 5). Such phenomenon is in agreement with the findings of our previous study on UV/PDS degradation of ACE [30]. Toth et al. [10] found that $^{\bullet}OH$ was more reactive with ACE than that of $SO_4^{\bullet-}$ based on the measurement of rate constants of ACE with $^{\bullet}OH$ and $SO_4^{\bullet-}$, which was (3.80 ± 0.27) × 10^9 and <2 × 10^7 respectively.

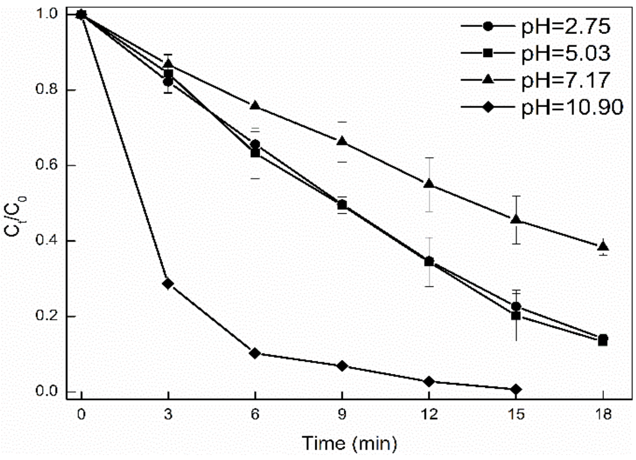

Fig. 3. Degradation of ACE by UV/PMS at different initial pH values (The average initial concentration of ACE was 4.79 ± 0.019 μM and $[PMS]_0$ = 25 μM).

3.4. Effects of HA and FA

HA and FA are ubiquitous components in natural waters that can influence the photochemical behaviors of organic pollutants. The roles of HA and FA at various concentrations on the removal of ACE by UV/PMS were evaluated, and the results are displayed in Fig. 6. ACE degradation by UV/PMS was reduced with the presence of HA or FA, and the inhibitory effect on ACE degradation with high concentration HA and FA was more significant. This is because HA and FA could serve as filters/screens to absorb/scatter UV radiation rather than the UV photons' being absorbed by PMS for radical generation or by ACE for direct photolysis [40,41]. Furthermore, HA and FA have been reported to be $^{\bullet}OH$ and $SO_4^{\bullet-}$ scavengers [42]. Giannakis et al. [18] suggested that $^{\bullet}OH$ reacted with dissolved organic matter at a rate around 2.8 × 10^8 M^{-1} s^{-1}, while $SO_4^{\bullet-}$ had relatively

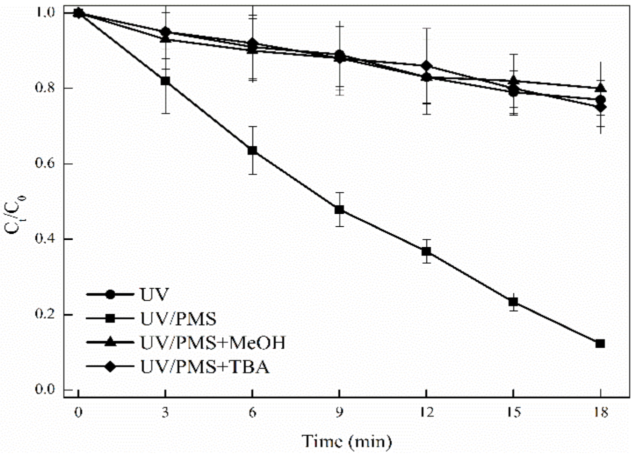

Fig. 4. Roles of MeOH and TBA on ACE degradation (the average initial concentration of ACE was 4.80 ± 0.013 μM, $[PMS]_0$ = 25 μM, and $[MeOH]_0$ = $[TBA]_0$ = 5 mM).

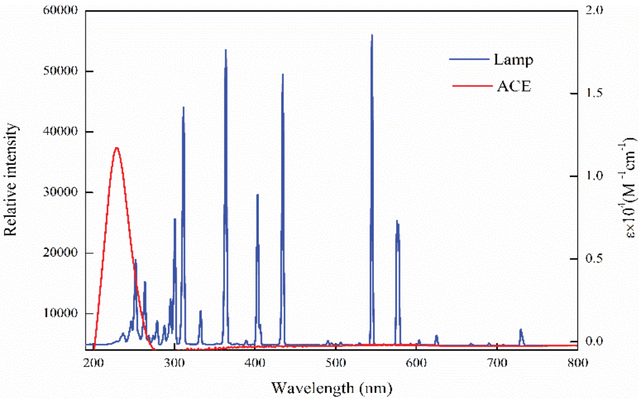

Fig. 5. The absorption spectra of ACE and the relative intensity of the light source used in the experiment (ε: molar absorption coefficient of ACE).

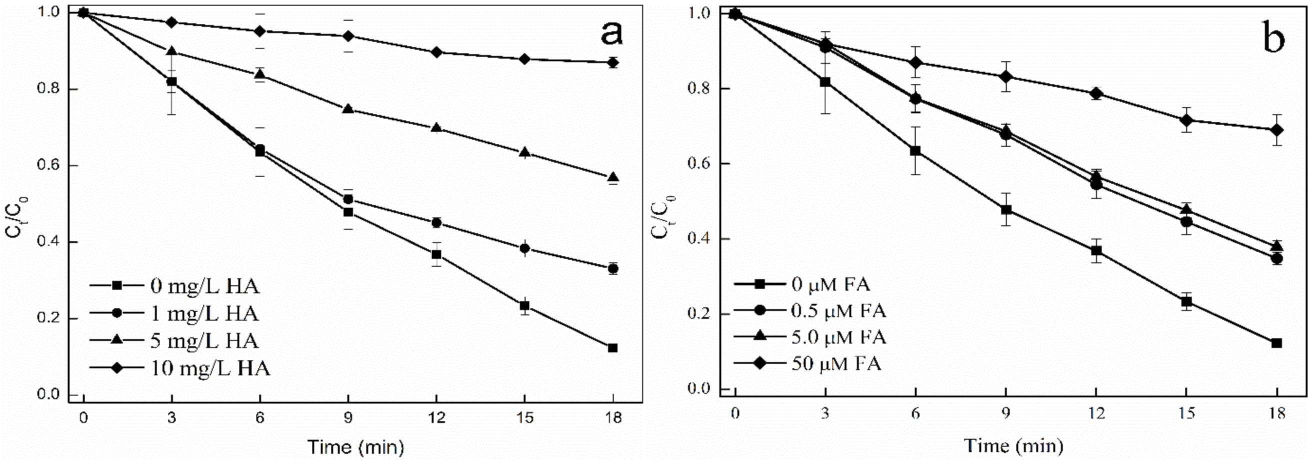

Fig. 6. UV/PMS degradation of ACE in the presence of HA (a) and FA (b) (a: average initial concentration of ACE was 4.64 ± 0.021 μM and $[PMS]_0$ = 25 μM; b: average initial concentration of ACE was 4.38 ± 0.072 μM and $[PMS]_0$ = 25 μM).

different rate with dissolved organic matter which was about 7.8 × 10^7 M^{-1} s^{-1}. Thus, the presence of HA and FA reduced ACE degradation, which was similar with that obtained during ACE degradation by UV/PDS [30].

3.5. Effect of inorganic anions

Natural waters are complex and contain inorganic ions such as HCO_3^-, Cl^-, and NO_3^-. The effects of these ions on ACE degradation by UV/PMS were investigated, and the results are presented in Fig. 7. HCO_3^- significantly reduced the degradation of ACE, Cl^- slightly reduced ACE degradation, and NO_3^- was beneficial for the removal of ACE.

HCO_3^- is a kind of $^\bullet OH$ and $SO_4^{\bullet-}$ scavenger, and less reactive species $CO_3^{\bullet-}$ and HCO_3 could be produced [Eqs. (2) and (3)] [43] causing a substantial reduction in ACE removal. The performance of HCO_3^- in UV/PMS degradation of ACE was similar to that in UV/PDS system [30].

$$HCO_3^- + {}^\bullet OH \rightarrow CO_3^{\bullet-} + H_2O \quad (2)$$

$$HCO_3^- + SO_4^{\bullet-} \rightarrow HCO_3^\bullet + SO_4^{2-} \quad (3)$$

Cl^- can also react with $^\bullet OH$ and $SO_4^{\bullet-}$ producing chlorine-containing radicals such as $ClOH^{\bullet-}$, $Cl^\bullet$, and $Cl_2^{\bullet-}$ with varying rate constants according to Eqs. (4)–(6) [42,44,45]. Therefore, $SO_4^{\bullet-}$ and $^\bullet OH$ may be scavenged by Cl^- resulting in reduced ACE removal.

$$Cl^- + {}^\bullet OH \leftrightarrow ClOH^{\bullet-} \qquad k = 3.0\text{–}4.3 \times 10^9\ M^{-1}\,s^{-1} \quad (4)$$

$$Cl^- + SO_4^{\bullet-} \rightarrow Cl^\bullet + SO_4^{2-} \qquad k = 1.3\text{–}6.6 \times 10^8\ M^{-1}\,s^{-1} \quad (5)$$

$$Cl^- + Cl^\bullet \rightarrow Cl_2^{\bullet-} \qquad k = 6.5 \times 10^9\ M^{-1}\,s^{-1}\text{–}2.1 \times 10^{10}\ M^{-1}\,s^{-1} \quad (6)$$

Of note, PMS can also directly react with chloride and bicarbonate and produce HOCl and HCO_4^- [Eqs. (7) and (8)] [43,46], which contributes to the reduced ACE removal.

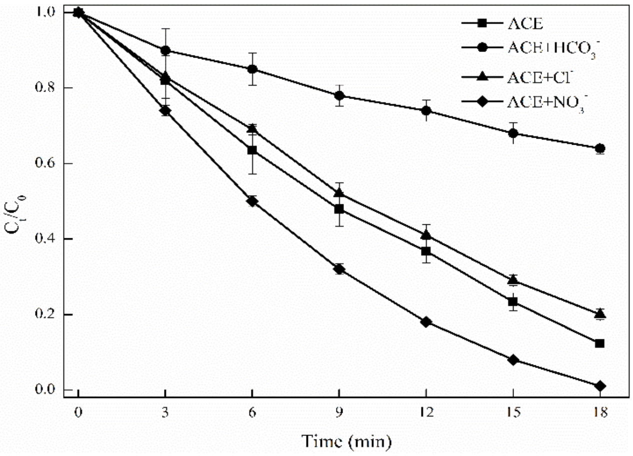

Fig. 7. UV/PMS degradation of ACE with the presence of inorganic ions (average initial concentration of ACE was 4.60 ± 0.044 μM, $[PMS]_0$ = 25 μM, and $[HCO_3^-]_0 = [Cl^-]_0 = [NO_3^-]_0$ = 1 mM).

$$HSO_5^- + Cl^- \rightarrow HOCl + SO_4^{2-} \quad (7)$$

$$HSO_5^- + HCO_3^- \rightarrow HCO_4^- + HSO_4^- \quad (8)$$

NO_3^- is a photosensitizer which can be photolyzed into $^\bullet OH$ under UV irradiation [47], resulting in enhanced ACE degradation by UV/PMS. Meanwhile, NO_3^- is also a nucleophilic reagent that can activate PMS to generate more reactive oxygen species, for example, $^\bullet OH$ [48], resulting in enhanced ACE degradation by UV/PMS as well. The performance of NO_3^- in UV/PMS degradation of ACE was similar to that in UV/PDS system [30].

3.6. Effect of water quality

To evaluate the feasibility of utilizing UV/PMS to treat real ACE-contaminated water, ACE degradation were conducted in both ultrapure water (UW) and SW. From Fig. 8, it can be seen that ACE degradation in SW was significantly reduced compared with that in UW. SW absorbs UV and can competitively absorb light. Therefore, ACE degradation was inhibited. Additionally, components of SW (HA, FA, and HCO_3^-) do not facilitate to ACE degradation. Overall, the performance of ACE degradation by UV/PMS was similar to the UV/PDS degradation of ACE [30].

3.7. Proposed ACE degradation mechanisms

In this section, high concentrations of PMS (250 μM) and ACE (50 μM) were used to obtain high signal of by-products, and UV irradiation was also prolonged as 35 min. Finally, four degradation products of ACE were identified (Table 2). The corresponding ACE degradation mechanisms were shown in Fig. 9.

Three by-products of ACE with m/z of 117, 165, and 170 were identical to our previous study on the degradation of ACE by UV/PDS [30], and the degradation pathways were also the same. In short, m/z 117, 165, and 170 were formed by oxidation, hydroxyl substitution, hydrolysis and hydration of ACE. In addition, another product m/z 106 was identified during the degradation of ACE by UV/PMS. Firstly, a transformation intermediate m/z 196 was formed via the oxidation of ACE, then it was oxidized to form glycerin (m/z 92), and glycerin was further oxidized to form glyceric acid (m/z 106). Punturat and Huang [49] also detected m/z 106 during the electrochemical degradation of ACE.

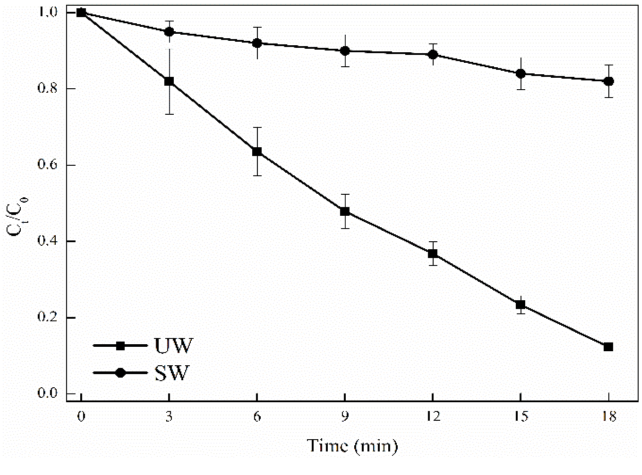

Fig. 8. Degradation of ACE by UV/PMS in natural water (average initial concentration of ACE was 4.79 ± 0.003 μM and $[PMS]_0 = 25$ μM).

Table 2
Degradation by-products of ACE by UV/PMS

m/z	Retention time (min)	Molecular formula	Relative peak intensity (%)	Degradation pathways
106	2.78	$C_3H_6O_4$	11.48	Oxidation
117	32.67	$C_4H_7NO_3$	38.70	Oxidation
165	1.49	$C_3H_3NO_5S$	100.00	Hydroxyl substitution
170	8.31	$C_2H_4NO_6S$	20.93	Oxidation, hydrolysis, and hydration

3.8. Comparison with UV/PDS and UV/H_2O_2

The degradation rate and mineralization degree of ACE by UV/PMS, UV/PDS, and UV/H_2O_2 are compared in Figs. 10 and 11. Due to the low TOC analyzer detection limit, the ACE concentration used in the mineralization experiments was high (48.95 μM in average), and the oxidant concentration was proportionally increased (250 μM). The results showed that both UV/PDS and UV/PMS have advantages over UV/H_2O_2 in degradation and mineralization of ACE, and the degradation ability of ACE by UV/PMS was inferior to that by UV/PDS. By fitting to the first-order reaction kinetics model, ACE degradation rate decreased as follows: UV/PDS (0.1551 min^{-1}) > UV/PMS (0.1469 min^{-1}) > UV/H_2O_2 (0.0340 min^{-1}). Khan et al. [34] investigated the degradation of atrazine and found that UV/PDS was the most efficient process, followed by UV/PMS and UV/H_2O_2. They ascribed this to the higher quantum yield of reactive radicals from UV/PDS, that is, 1.8 compared to 1.04 for UV/PMS and 1.0 for UV/H_2O_2 [41].

While, the order of the mineralization rate of ACE was in the order of UV/PDS (0.0080 min^{-1}) > UV/PMS (0.0047 min^{-1}) > UV/H_2O_2 (0.0028 min^{-1}). Anipsitakis and Dionysiou [26] also found a similar mineralization ability for 2,4-dichlorophenol, with the mineralization degree in 4 h in the order of UV/PDS (82%) > UV/PMS (74%) > UV/H_2O_2 (67%), which is in accordance with ours. They explained this by the fact that the UV absorption of these oxidants followed the order of PDS > PMS > H_2O_2.

4. Conclusion

This work demonstrated that ACE can be substantially degraded by the UV/PMS process. The degradation process of ACE obeyed to the first-order kinetics equation. The ACE reaction rate decreased with the increasing initial concentration of ACE, but increased with increasing initial concentration of PMS. Both acidic and alkaline conditions were suitable for ACE degradation. The presence of HA and FA reduced the degradation of ACE. Inorganic anions had different effects on ACE degradation, with promoting effect of NO_3^- and inhibitory effects of HCO_3^- and Cl^-. In natural water, ACE degradation was also inhibited. Four degradation products of ACE were identified through the UPLC/TOF-MS analysis, and the proposed major degradation mechanisms were oxidation, hydroxyl substitution, hydrolysis, and hydration. $^•OH$ played a primary role in ACE degradation by UV/PMS. UV/PMS was more favorable than UV/H_2O_2 for the removal of ACE, although the performance of UV/PMS in removal of ACE was inferior to that by UV/PDS.

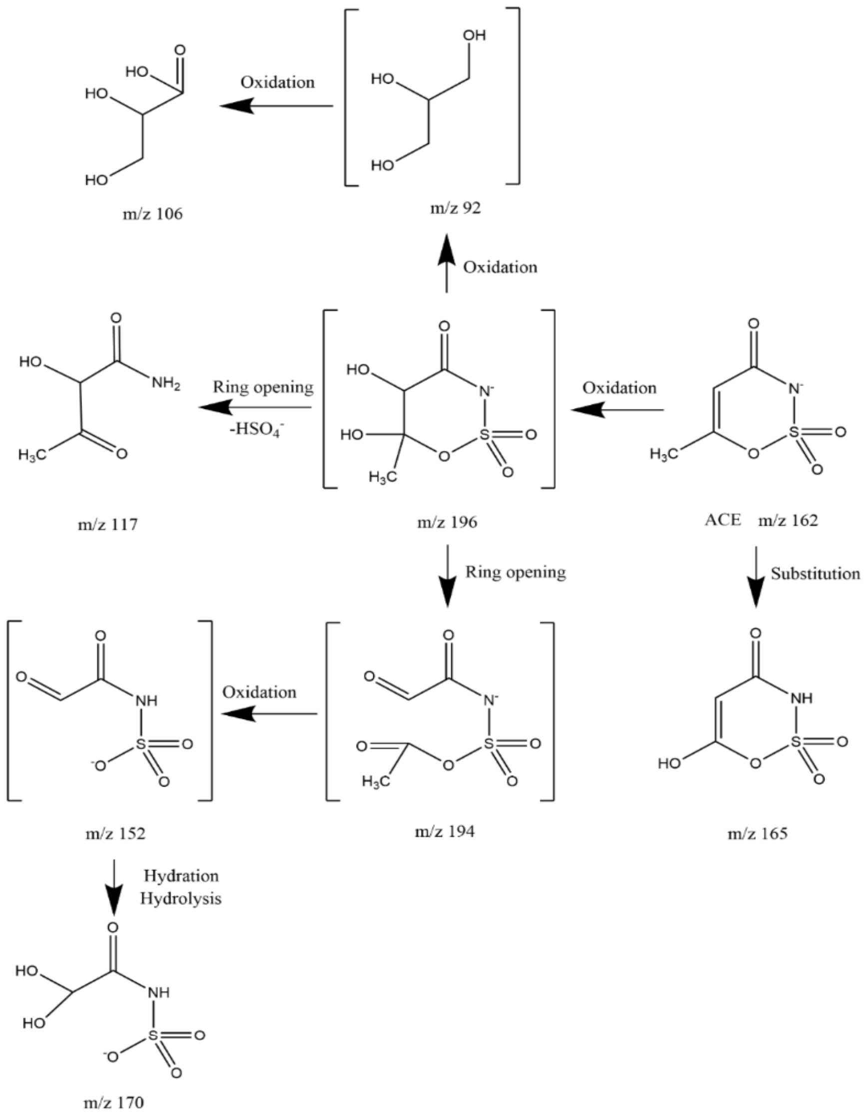

Fig. 9. ACE degradation mechanisms by UV/PMS (Intermediate products are shown in brackets).

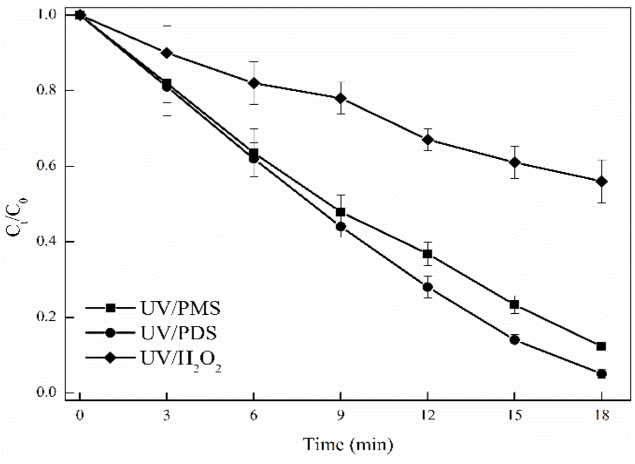

Fig. 10. ACE degradation by UV/PMS, UV/PDS, and UV/H_2O_2 (average initial concentration of ACE was 4.78 ± 0.007 μM and $[PMS]_0 = [PDS]_0 = [H_2O_2]_0 = 25$ μM).

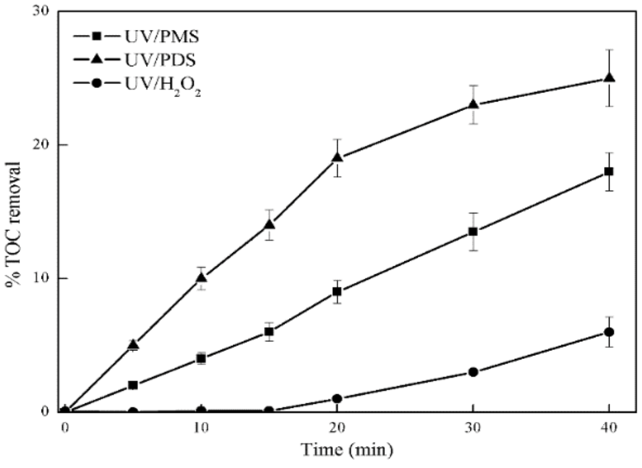

Fig. 11. ACE mineralization by UV/PMS, UV/PDS, and UV/H_2O_2 (average initial concentration of ACE was 48.95 ± 0.43 μM and $[PMS]_0 = [PDS]_0 = [H_2O_2]_0 = 250$ μM).

Acknowledgements

This work was supported by the National Natural Science Foundation of China (Grant No. 41403101); Department of Science and Technology of Jilin Province (Grant No. 20190303059SF, 20190303092SF and 20200403004SF); Jilin Province Development and Reform Commission (Grant No. 2019C056-6); China Scholarship Council and Innovation and Entrepreneurship Training Program for College Students in Jilin Province (S202110191111).

References

[1] M. Wu, Y. Qian, J.M. Boyd, S.E. Hrudey, X.C. Le, X.-F. Li, Direct large volume injection ultra-high performance liquid chromatography-tandem mass spectrometry determination of artificial sweeteners sucralose and acesulfame in well water, J. Chromatogr. A, 1359 (2014) 156–161.

[2] I.J. Buerge, H.R. Buser, M. Kahle, M.D. Muller, T. Poiger, Ubiquitous occurrence of the artificial sweetener acesulfame in the aquatic environment: an ideal chemical marker of domestic wastewater in groundwater, Environ. Sci. Technol., 43 (2009) 4381–4385.

[3] M. Scheurer, M. Godejohann, A. Wick, O. Happel, T.A. Ternes, H.J. Brauch, W.K.L. Ruck, F.T. Lange. Structural elucidation of main ozonation products of the artificial sweeteners cyclamate and acesulfame, Environ. Sci. Pollut. Res., 19 (2012) 1107–1118.

[4] Z. Sang, Y. Jiang, Y.K. Tsoi, K.S.Y. Leung, Evaluating the environmental impact of artificial sweeteners: a study of their distributions, photodegradation and toxicities, Water Res., 52 (2014) 260–274.

[5] M. Scheurer, H.J. Brauch, F.T. Lange, Analysis and occurrence of seven artificial sweeteners in german waste water and surface water and in soil aquifer treatment (SAT), Anal. Bioanal. Chem., 394 (2009) 1585–1594.

[6] Y. Xu, Z.Y. Lin, Y. Wang, H. Zhang, The UV/peroxymonosulfate process for the mineralization of artificial sweetener sucralose, Chem. Eng. J., 317 (2017) 561–569.

[7] C. Luo, J. Gao, D. Wu, J. Jiang, Y. Liu, W. Zhou, J. Ma, Oxidation of 2,4-bromophenol by UV/PDS and formation of bromate and brominated products: a comparison to UV/H_2O_2, Chem. Eng. J., 358 (2019) 1342–1350.

[8] Y. Shao, Z.C. Pang, L.L. Wang, X.W. Liu, Efficient degradation of acesulfame by ozone/peroxymonosulfate advanced oxidation process, Molecules, 24 (2019) 2874, doi: 10.3390/molecules24162874.

[9] B. Atrayee, G. Sarbani, M. Anita, Genotoxicity testing of low-calorie sweeteners: aspartame, acesulfame-K, and saccharin, Drug Chem. Toxicol., 31 (2008) 447–457.

[10] J.E. Toth, K.A. Rickman, A.R. Venter, J.J. Kiddle, S.P. Mezyk, Reaction kinetics and efficiencies for the hydroxyl and sulfate radical based oxidation of artificial sweeteners in water, J. Phys. Chem. A, 116 (2012) 9819–9824.

[11] H. Sun, S. Wang, Catalytic oxidation of organic pollutants in aqueous solution using sulfate radicals, Catalysis, 27 (2015) 209–247.

[12] F. Ghanbari, M. Moradi, Application of peroxymonosulfate and its activation methods for degradation of environmental organic pollutants, Chem. Eng. J., 310 (2017) 41–62.

[13] B.T. Zhang, Y. Zhang, Y. Teng, M. Fan, Sulfate radical and its application in decontamination technologies, Crit. Rev. Env. Sci. Technol., 45 (2015) 1756–1800.

[14] J.L. Wang, S.Z. Wang, Activation of persulfate (PS) and peroxymonosulfate (PMS) and application for the degradation of emerging contaminants, Chem. Eng. J., 334 (2018) 1502–1517.

[15] J.A. Khan, X. He, H.M. Khan, N.S. Shah, D.D. Dionysiou, Oxidative degradation of atrazine in aqueous solution by UV/H_2O_2/Fe^{2+}, UV/$S_2O_8^{2-}$/Fe^{2+} and UV/HSO_5^-/Fe^{2+} processes: a comparative study, Chem. Eng. J., 218 (2013) 376–383.

[16] G.P. Anipsitakis, D.D. Dionysiou, Radical generation by the interaction of transition metals with common oxidants, Environ. Sci. Technol., 38 (2004) 3705–3712.

[17] Q. Zhao, Q. Mao, Y. Zhou, J. Wei, X. Liu, J. Yang, L. Luo, J. Zhang, H. Chen, H. Chen. Metal-free carbon materials-catalyzed sulfate radical-based advanced oxidation processes: a review on heterogeneous catalysts and applications, Chemosphere, 189 (2017) 224–238.

[18] S. Giannakis, K.Y.A. Lin, F. Ghanbari, A review of the recent advances on the treatment of industrial wastewaters by sulfate radical-based advanced oxidation processes (SR-AOPs), Chem. Eng. J., 406 (2020) 127083, doi: 10.1016/j.cej.2020.127083.

[19] W. Zhang, S. Zhou, J. Sun, X. Meng, J. Luo, D. Zhou, J. Crittenden, Impact of chloride ions on UV/H_2O_2 and UV/persulfate advanced oxidation processes, Environ. Sci. Technol., 52 (2018) 7380–7389.

[20] J. Sharma, I.M. Mishra, D.D. Dionysiou, V. Kumar, Oxidative removal of Bisphenol A by UV-C/peroxymonosulfate (PMS): kinetics, influence of co-existing chemicals and degradation pathway, Chem. Eng. J., 276 (2015) 193–204.

[21] Y.M. Qi, R.J. Qu, J.Q. Liu, J. Chen, G. Al-Basher, N. Alsultan, Z.Y. Wang, Z.L. Huo, Oxidation of flumequine in aqueous solution by UV-activated peroxymonosulfate: kinetics, water matrix effects, degradation products and reaction pathways, Chemosphere, 237 (2019) 124484, doi: 10.1016/j.chemosphere.2019.124484.

[22] T. Olmez-Hanci, C. Imren, I. Kabdaşli, O. Tünay, I. Arslan-Alaton, Application of the UV-C photo-assisted peroxymonosulfate oxidation for the mineralization of dimethyl phthalate in aqueous solutions, Photochem. Photobiol. Sci., 10 (2011) 408–413.

[23] S. Yang, P. Wang, X. Yang, L. Shan, W. Zhang, X. Shao, J.L. Shi, H.J. Liu, G.X. Yan, G.G. Liu, S.X. Gao, Z.G. Gao, Degradation efficiencies of azo dye Acid Orange 7 by the interaction of heat, UV and anions with common oxidants: persulfate, peroxymonosulfate and hydrogen peroxide, J. Hazard. Mater., 179 (2010) 552–558.

[24] C. Cai, H. Zhang, X. Zhong, L. Hou, Ultrasound enhanced heterogeneous activation of peroxymonosulfate by a bimetallic Fe–Co/SBA-15 catalyst for the degradation of Orange II in water, J. Hazard. Mater., 283 (2015) 70–79.

[25] J.B. Peng, Z.L. Wang, S.Y. Wang, J. Liu, Y.Z. Zhang, B.J. Wang, Z.M. Gong, M.J. Wang, H. Dong, Enhanced removal of methylparaben mediated by cobalt/carbon nanotubes (Co/CNTs) activated peroxymonosulfate in chloride-containing water: Reaction kinetics, mechanisms and pathways, Chem. Eng. J., 409 (2021) 128176.

[26] G.P. Anipsitakis, D.D. Dionysiou, Degradation of organic contaminants in water with sulfate radicals generated by the conjunction of peroxymonosulfate with cobalt, Environ. Sci. Technol., 37 (2003) 4790–4797.

[27] F. Ji, C. Li, X. Wei, J. Yu, Efficient performance of porous Fe_2O_3 in heterogeneous activation of peroxymonosulfate for decolorization of Rhodamine B, Chem. Eng. J., 231 (2013) 434–440.

[28] S. Li, Y. Ren, Y. Fu, X. Gao, C. Jiang, G. Wu, H.Q. Ren, J.J. Geng, Fate of artificial sweeteners through wastewater treatment plants and water treatment processes, PLoS One, 13 (2018) e0189867, doi: 10.1371/journal.pone.0189867.

[29] Z. Wang, G.N.S.T. Thuy, V. Srivastava, I. Ambat, M. Sillanpää, Photocatalytic degradation of an artificial sweetener (Acesulfame-K) from synthetic wastewater under UV-LED controlled illumination, Process Saf. Environ. Prot., 123 (2019) 206–214.

[30] H. Xue, S. Gao, M. Li, Y. Wang, B. Liu, Performance of ultraviolet/persulfate process in degrading artificial sweetener acesulfame, Environ. Res., 188 (2020) 109804, doi: 10.1016/j.envres.2020.109804.

[31] H. Xue, W. Chen, M. Li, B. Liu, G. Li, X. Han, Assessment of major ions and trace elements in snow: a case study across northeastern China, 2017–2018, Chemosphere, 251 (2020) 126328, doi: doi: 10.1016/j.chemosphere.2020.126328.

[32] J. Zou, Y. Huang, L. Zhu, Z. Cui, B.L. Yuan, Multi-wavelength spectrophotometric measurement of persulfates using 2,2′-azino-bis(3-ethylbenzothiazoline-6-sulfonate) (ABTS) as indicator, Spectrochim. Acta, Part A, 216 (2019) 214–220.

[33] K. Fedorov, M. Plata-Gryl, J. Khan, G. Boczkaj, Ultrasound-assisted heterogeneous activation of persulfate and peroxymonosulfate by asphaltenes for the degradation of BTEX in water, J. Hazard. Mater., 397 (2020) 122804, doi: 10.1016/j.jhazmat.2020.122804.

[34] J.A. Khan, X. He, N.S. Shah, H.M. Khan, E. Hapeshi, D. Fatta-Kassinos, D.D. Dionysiou, Kinetic and mechanism investigation on the photochemical degradation of atrazine with activated H_2O_2, $S_2O_8^{2-}$ and HSO_5^-, Chem. Eng. J., 252 (2014) 393–403.

[35] X. Xu, J. Chen, R. Qu, Z. Wang, Oxidation of Tris (2-chloroethyl) phosphate in aqueous solution by UV-activated peroxymonosulfate: kinetics, water matrix effects, degradation products and reaction pathways, Chemosphere, 185 (2017) 833–843.

[36] C. Liang, H.-W. Su, Identification of sulfate and hydroxyl radicals in thermally activated persulfate, Ind. Eng. Chem. Res., 48 (2009) 5558–5562.

[37] M. Zou, Y. Qi, R. Qu, G. Al-Basher, X. Pan, Z. Wang, Z.L. Huo, F. Zhu, Effective degradation of 2,4-dihydroxybenzophenone by zero-valent iron powder (Fe^0)-activated persulfate in aqueous solution: kinetic study, product identification and theoretical calculations, Sci. Total Environ., 771 (2021) 144743, doi: 10.1016/j.scitotenv.2020.144743.

[38] Y.-H. Guan, J. Ma, X.-C. Li, J.-Y. Fang, L.-W. Chen, Influence of pH on the formation of sulfate and hydroxyl radicals in the UV/Peroxymonosulfate system, Environ. Sci. Technol., 45 (2011) 9308–9314.

[39] Y. Fu, G. Wu, J. Geng, J. Li, S. Li, H. Ren, Kinetics and modeling of artificial sweeteners degradation in wastewater by the UV/Persulfate process, Water Res., 150 (2019) 12–20.

[40] S. Li, J. Hu, Photolytic and photocatalytic degradation of tetracycline: Effect of humic acid on degradation kinetics and mechanisms, J. Hazard. Mater., 318 (2016) 134–144.

[41] J.A. Khan, X. He, N.S. Shah, M. Sayed, H.M. Khan, D.D. Dionysiou, Degradation kinetics and mechanism of desethyl-atrazine and desisopropyl-atrazine in water with $^{\bullet}OH$ and $SO_4^{\bullet-}$ based-AOPs, Chem. Eng. J., 325 (2017) 485–494.

[42] M. Xu, J. Deng, A. Cai, X. Ma, X. Li, Comparison of UVC and UVC/Persulfate processes for tetracycline removal in water, Chem. Eng. J., 384 (2020) 123320, doi: 10.1016/j.cej.2019.123320.

[43] S. Yang, J. Zhang, Q. Han, L. Feng, Influence of HCO_3^- on the degradation of azo dye acid orange 7 by CO^{2+}/HSO_5^- system, Environ. Chem., 33 (2014) 500–507 (In Chinese).

[44] S. Wacawek, H.V. Lutze, K. Grübel, V. Padil, D.D. Dionysiou, Chemistry of persulfates in water and wastewater treatment: a review, Chem. Eng. J., 330 (2017) 44–62.

[45] B. Nikravesh, A. Shomalnasab, A. Nayyer, N. Aghababaei, F. Ghanbari, UV/Chlorine process for dye degradation in aqueous solution: mechanism, affecting factors and toxicity evaluation for textile wastewater, J. Environ. Chem. Eng., 8 (2020) 104244, doi: 10.1016/j.jece.2020.104244.

[46] F. Ghanbari, M. Khatebasreh, M. Mahdavianpour, K. Lin, Oxidative removal of benzotriazole using peroxymonosulfate/ozone/ultrasound: synergy, optimization, degradation intermediates and utilizing for real wastewater, Chemosphere, 244 (2020) 125326, doi: 10.1016/j.chemosphere.2019.125326.

[47] K. Mostofa, C.Q. Liu, H. Sakugawa, D. Vione, M.A. Mottaleb, Photoinduced Generation of Hydroxyl Radical in Natural Waters, Springer, Berlin, Heidelberg, 2013.

[48] U. Kalsoom, S.S. Ashraf, M.A. Meetani, M.A. Rauf, H.N. Bhatti, Degradation and kinetics of H_2O_2 assisted photochemical oxidation of remazol turquoise blue, Chem. Eng. J., 200–202 (2012) 373–379.

[49] V. Punturat, K.L. Huang, Degradation pathways and organic matter transformation of acesulfame potassium electro-oxidation in real water matrices, J. Taiwan Inst. Chem. Eng., 80 (2017) 222–230.